

Article

Zbed3 participates in the subcortical maternal complex and regulates the distribution of organelles

Zheng Gao^{1,2,†}, Xiaoxin Zhang^{1,†}, Xingjiang Yu¹, Dandan Qin¹, Yi Xiao¹, Yang Yu¹, Yunlong Xiang¹, Xiaoqing Nie¹, Xukun Lu¹, Wenbo Liu¹, Zhaohong Yi³, and Lei Li^{1,2,*}

¹ State Key Laboratory of Stem Cell and Reproductive Biology, Institute of Zoology, Chinese Academy of Sciences, Beijing 100101, China

² University of Chinese Academy of Sciences, Beijing 100049, China

³ Key Laboratory of Urban Agriculture (North) of Ministry of Agriculture, College of Biological Science and Engineering, Beijing University of Agriculture, Beijing 102206, China

[†] These authors contributed equally to this work.

* Correspondence to: Lei Li, E-mail: lil@ioz.ac.cn

We previously identified a subcortical maternal complex (SCMC) that is essential for early embryogenesis and female fertility in mice. However, the molecular mechanism by which the SCMC affects female fertility remains largely uncharacterized. Here, we report that a novel maternal protein, zinc finger BED-type containing 3 (Zbed3), participates in the SCMC. Depletion of maternal *Zbed3* results in reduced fecundity of females, because of the impaired and delayed development in a proportion of mutant embryos. The loss of maternal *Zbed3* results in asymmetric zygotic division and abnormal distributions of organelles in the affected oocytes and zygotes, similar to the phenotypes observed in females with disrupted core SCMC genes. Further investigation revealed that these phenotypes are associated with disrupted dynamics of microtubules and/or formation of cytoplasmic lattices (CPLs). The stability and localization of *Zbed3* depend on, but are not required for, the formation of the SCMC. Thus, our data suggest *Zbed3* as one of downstream proteins mediating SCMC functions and provide further insights into the roles of the SCMC and CPLs in female fertility.

Keywords: Zbed3, SCMC, organelle distribution, maternal effect gene, cytoskeleton, early embryogenesis, cytoplasmic lattices

Introduction

The hiatus of transcriptional activity of zygotic genome activation (ZGA) from mature gametes to early embryos and unequal burden of gametes in early embryogenesis dictate essential roles of maternal effect genes in animal development (Li et al., 2010, 2013). Since the first report of the maternal effect gene (*Dorsal*) in animals in the 1980s, hundreds of these genes have been characterized for their important roles, including but not limited to cell fate determination, body axis establishment, and ZGA of early embryonic development in *Drosophila melanogaster* (Stein and Stevens, 2014). In mammals, it was until 2000 when the first maternal effect gene *Mater* (official symbol, *Nlrp5*) was reported (Tong et al., 2000). Mouse genetics have documented that maternal effect genes function in multiple processes, including DNA damage repair and replication, epigenetic

reprogramming, the first cell division, clearance of maternal materials, ZGA, and cleavage stage embryogenesis (Li et al., 2010, 2013; Gu et al., 2011; Lin et al., 2014; Yu et al., 2014, 2016; Xu et al., 2015; Liu et al., 2016). However, the molecular events of maternal regulation in early mammalian embryonic development have not been well established.

We previously identified a subcortical maternal complex (SCMC) that is an oocyte–early embryo-specific protein complex critical for mouse embryogenesis (Li et al., 2008b). This complex includes at least four maternal proteins: Mater (official symbol, *Nlrp5*), Floped (official symbol, *Ooep*), Filia (official symbol, *Khdc3*), and Tle6 (Tong et al., 2000; Herr et al., 2008; Ohsugi et al., 2008). The formation of the SCMC depends on Mater, Floped, and Tle6, but not Filia, suggesting that these three proteins are the core components of the complex (Yu et al., 2014). The three core proteins bind to each other and function as a whole to control the symmetric division of mouse zygotes by regulating F-actin dynamics (Li et al., 2008b; Yu et al., 2014). Disruption of SCMC core proteins in mice results in similar

Received March 21, 2017. Revised April 14, 2017. Accepted April 29, 2017.
© The Author (2017). Published by Oxford University Press on behalf of *Journal of Molecular Cell Biology*, IBCB, SIBS, CAS. All rights reserved.

phenotypes that encompass asymmetric division of zygotes, developmental arrest at 2-cell embryos, and female infertile (Tong et al., 2000; Li et al., 2008b; Yu et al., 2014), while depletion of Filia leads to aneuploidy of early embryos and female subfertility (Zheng and Dean, 2009). Recently, SCMC components were shown to be involved in the formation of cytoplasmic lattices (CPLs) (Kim et al., 2010, 2014; Tashiro et al., 2010; Monti et al., 2013). The SCMC is conserved in mammals including humans (Bebbere et al., 2014; Zhu et al., 2015). The mutant SCMC genes have been reported to be related to human reproductive disorders (Parry et al., 2011; Alazami et al., 2015; Docherty et al., 2015). Currently, the clarification of molecular mechanisms of the SCMC represents a milestone to understand the comprehension of maternal regulatory network and oocyte biology in mammals (Li and Albertini, 2013; Bebbere et al., 2016).

The SCMC has a much larger molecular mass (>669 kDa) than the summation of all known SCMC proteins (~270 kDa) (Li et al., 2008b), implying other proteins involved in the complex. In this study, we identified zinc finger BED-type containing 3 (Zbed3) as a novel component of the SCMC. Zbed3 contains a zinc finger BED domain and belongs to ZBED family of proteins (Hayward et al., 2013). However, the physiological function of this gene is unknown. Through established *Zbed3* mutant mice, we found that Zbed3 functions as the downstream protein of the SCMC to regulate organelle distributions via cytoskeleton and/or CPLs during mouse oocyte to zygote transition.

Results

Zbed3 is a novel component of the SCMC

To identify novel components of the SCMC, we collected ~3000 GV and MII eggs for co-immunoprecipitation (co-IP) with mouse anti-Tle6 monoclonal antibody. After separation of the precipitated proteins using SDS-PAGE, the polyacrylamide gel was stained with silver staining and analyzed with mass spectrometry (Figure 1A; Materials and methods). Based on the criterion that at least two unique peptides were present in the mouse anti-Tle6 antibody sample but absent in the control, we identified 23 proteins including all of the four previously identified SCMC proteins and a novel protein, Zbed3 (Supplementary Figure S1A).

To confirm these results, mouse anti-Tle6 or anti-Mater monoclonal antibodies were used to pull down the SCMC complex from normal mouse oocyte lysates. Both antibodies precipitated Zbed3, in addition to the known SCMC proteins (Figure 1B). Immunofluorescence staining showed that Zbed3 was diffused in the cytoplasm of GV oocytes, and gradually concentrated in the subcortex of MII oocytes. Zbed3 partially co-localized with Mater in both cytoplasmic and subcortical regions (Figure 1C). To examine the physical interaction between Zbed3 and the SCMC, we co-expressed 3× Flag-Zbed3 with four HA-tagged proteins or Myc-Mater in HEK-293T cells and performed co-IP experiments. Immunoblots showed that only Mater bound to Zbed3 (Figure 1D and Supplementary Figure S1B). Those results suggest that Zbed3 participates in the SCMC by interacting with

Mater. Thus, we characterized Zbed3 as a novel component of the SCMC.

Zbed3 exhibits a maternal expression pattern in mouse early development

Quantitative RT-PCR (qRT-PCR) showed that *Zbed3* mRNA was highly expressed in mouse ovary and testis, and was also present in other tissues (Figure 2A). However, immunoblots and immunofluorescence staining showed that Zbed3 was restricted to the cytoplasm of oocytes at different developmental stages in mouse ovary (Figure 2B and C). *Zbed3* transcripts were highly abundant from the GV stage of oogenesis to 1-cell zygotes, and then dramatically declined in 2-cell and the later stages of embryogenesis (Figure 2D). Thus, the expression profile of *Zbed3* is typical pattern of maternal effect genes. The level of Zbed3 appeared slightly increased after the 1-cell stage, and abruptly decreased in blastocysts (Figure 2E). Immunofluorescence staining showed that Zbed3 was localized in the cytoplasm, and concentrated in the subcortex of zygote and morula after fertilization (Figure 2F).

Maternal Zbed3 is important for early embryogenesis and fecundity of females

To investigate the physiological function of *Zbed3*, we established a line of *Zbed3* knockout mice (Supplementary Figure S2A–D; Materials and methods). We determined the fertility of *Zbed3*^{Δ/Δ} mice by measuring their litter sizes (mean ± SEM, litters) following a designed mating strategy (Figure 3A and Supplementary Figure S3A). *Zbed3*^{Δ/Δ} males exhibited normal fertility, compared with that of *Zbed3*^{+Δ} males. However, the litter sizes of *Zbed3*^{Δ/Δ} females (5.4 ± 2.1, *n* = 36) were statistically less than those from *Zbed3*^{+Δ} females (7.9 ± 2.9, *n* = 31), when mated with *Zbed3*^{+Δ} males (Figure 3A). Similar results were obtained from *Zbed3*^{Δ/Δ} females (5.1 ± 1.9, *n* = 9) mated with *Zbed3*^{Δ/Δ} males (Figure 3A). The phenotype of decreased pups in *Zbed3*^{Δ/Δ} females was not rescued (5.2 ± 0.8, *n* = 6) by mating with wild-type (wt) male mice, whose spermatozoa did not contribute Zbed3 to zygotes (Supplementary Figure S3B). This result was similar to that observed in maternal *Tle6*-null embryos (Supplementary Figure S3C). In our next experiments, unless otherwise stated, control (*Zbed3*^{+Δ}) and maternal knockout embryos from *Zbed3*^{Δ/Δ} females mated with wt (*Zbed3*^{+Δ/+}) male mice are labeled as ♀*Zbed3*^{+Δ} × ♂*Zbed3*^{+Δ/+} and ♀*Zbed3*^{Δ/Δ} × ♂*Zbed3*^{+Δ/+}, respectively (Supplementary Figure S3A). Overall, these results demonstrate that maternal *Zbed3* is important for the fecundity of female mice.

To determine the time of embryonic loss, we compared the number of preimplantation embryos in *Zbed3*^{+Δ} (control) and *Zbed3*^{Δ/Δ} females by mated with wt males. The numbers of zygotes (25.44 ± 2.1, *n* = 9 females) and 2-cell embryos (27.75 ± 3.77, *n* = 8) obtained from *Zbed3*^{Δ/Δ} females were comparable to those from *Zbed3*^{+Δ} females (zygotes: 26.11 ± 3.52, *n* = 7; 2-cell embryos: 26.44 ± 3.20, *n* = 9) at E0.5 and E1.5, respectively (Figure 3B). However, at E2.5, fewer >8 cells morulae (10.38 ± 1.70, *n* = 8) were isolated from *Zbed3*^{Δ/Δ} females, compared with

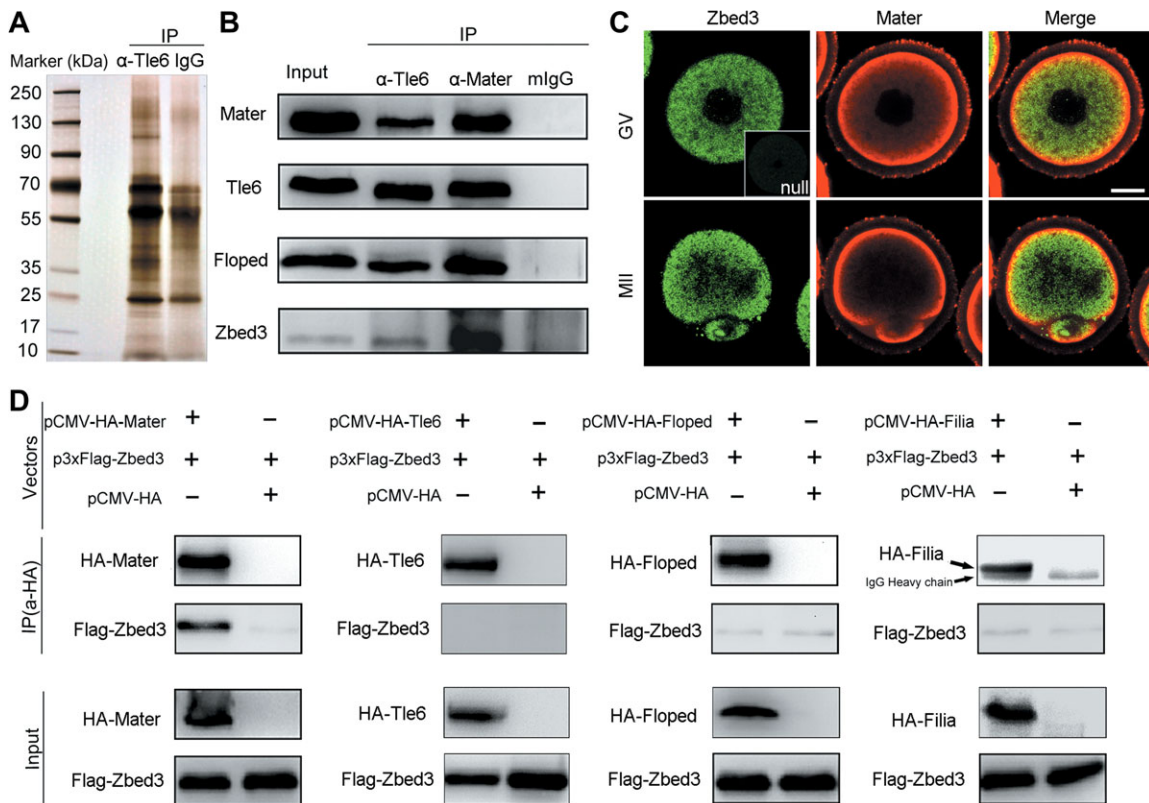


Figure 1 Zbed3 is a novel component of the SCMC. **(A)** The immunoprecipitates pulled down by anti-Tle6 antibody and mouse IgG were separated by SDS-PAGE and stained with silver staining. **(B)** The immunoprecipitates pulled down by anti-Tle6 antibody (α -Tle6), anti-Mater antibody (α -Mater), or mouse IgG from normal oocyte lysates (200 eggs) were immunoblotted for detecting Mater, Tle6, Floped, and Zbed3. The lysate of 20 eggs was used as input. **(C)** The GV and MII stage oocytes were examined by immunofluorescence staining for Zbed3 and Mater. A Zbed3-null oocyte in white box is as a negative control. Scale bar, 20 μ m. **(D)** Immunoprecipitates from co-IP performed with anti-HA antibody on cells co-expressing 3 \times FLAG-Zbed3 and HA-Mater, HA-Tle6, HA-Floped, or HA-Filia were immunoblotted, respectively. pCMV-HA with 3 \times FLAG-Zbed3 was used as a negative control. The bands (\sim 55 kDa) below HA-Filia are mouse IgG heavy chains.

Zbed3^{+/-} females (16.33 ± 1.79 , $n = 9$) (Figure 3B and C). At E3.5, the number of embryos with blastocoel recovered from Zbed3^{+/-} females (7.88 ± 0.58 , $n = 8$) was significantly less than those recovered from the controls (15.75 ± 2.19 , $n = 8$) (Figure 3B and C). We then cultured 2-cell embryos from Zbed3^{+/-} and control females *in vitro* and monitored the development of these embryos every 3 h. The results confirmed the delayed development of maternal Zbed3-null embryos after 2-cell stage (Figure 3D). Altogether, these data demonstrate that disruption of maternal Zbed3 causes impaired and delayed development of 2-cell embryos.

Maternal Zbed3 deficiency increases the number of 2-cell embryos with asymmetric blastomeres

Although the number of 2-cell embryos was comparable to the control, we observed a large number of 2-cell embryos recovered from Zbed3^{+/-} females exhibited asymmetric blastomeres (Figure 3E). To estimate the proportion of 2-cell embryos with asymmetric blastomeres, we stained F-actin with phalloidin to outline the 2-cell embryos, and measured the maximum cross-sectional areas of individual blastomeres. We defined two

blastomeres as asymmetric if the difference between their cross-sectional areas was greater than 10% (Yu et al., 2014). The percentage of asymmetric 2-cell embryos from Zbed3^{+/-} females ($55\% \pm 5.6\%$, $n = 112$ embryos) was significantly higher than those from Zbed3^{+/-} females ($21\% \pm 3.9\%$, $n = 85$) (Figure 3F). Those results imply that maternal Zbed3-null zygotes tend to divide asymmetrically.

To determine the spindle position, we cultured mouse zygotes to the metaphase stage and stained the spindles and chromosomes. We then measured the average distance between the chromosomes and the cellular center along the long axis of the spindle (Figure 3G). The average distance in zygotes from Zbed3^{+/-} females ($2.80 \pm 0.37 \mu$ m, $n = 27$) was larger than that in the controls ($1.46 \pm 0.17 \mu$ m, $n = 23$) (Figure 3H). These results indicate that maternal Zbed3 deficiency impairs the central position of the spindle, resulting in asymmetric division of mouse zygotes.

F-actin is disordered in maternal Zbed3-null zygotes

F-actin has been reported to be a regulator for symmetrical division in mouse zygotes (Chaigne et al., 2016). We detected

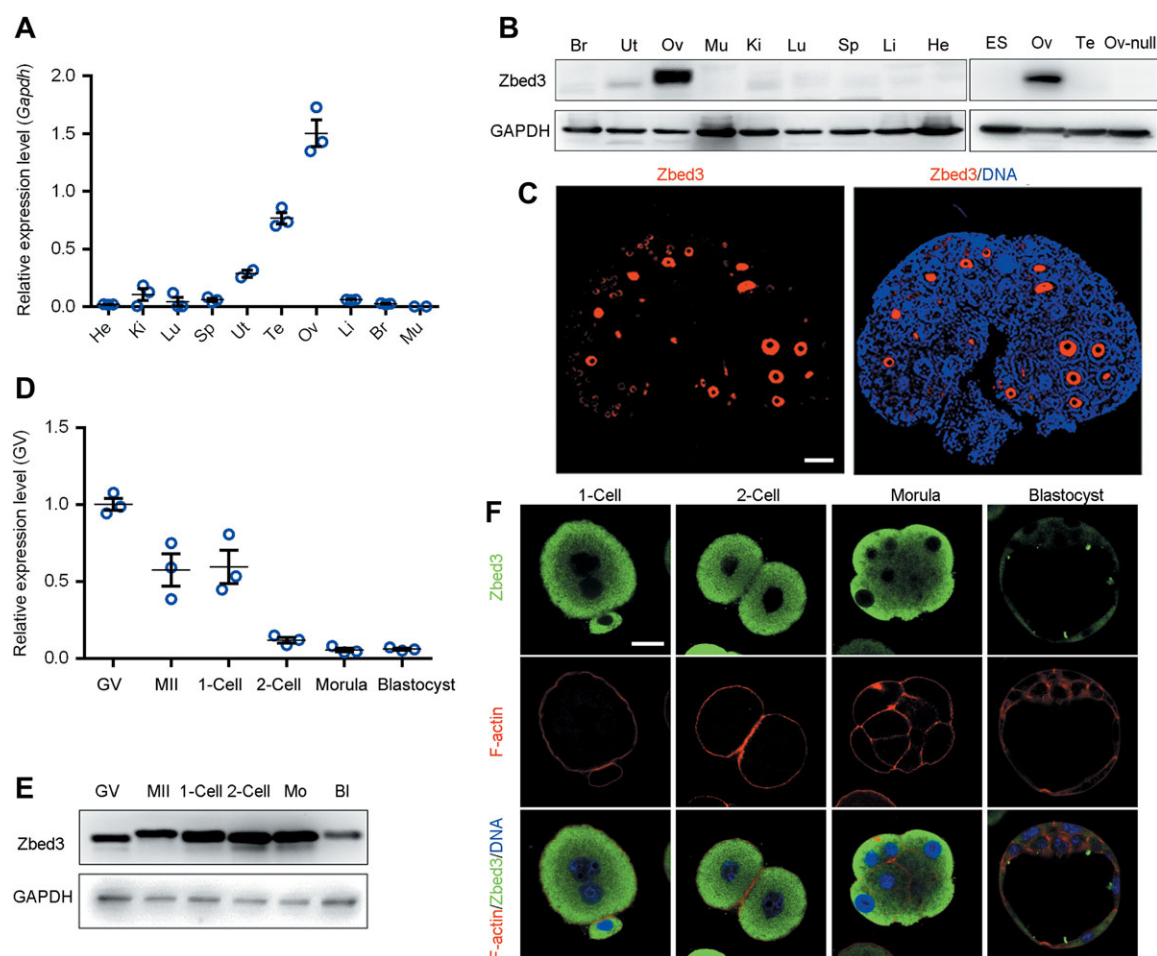


Figure 2 *Zbed3* exhibits a maternal expression profile. (A) The relative expression of *Zbed3* in mouse tissues was detected by qRT-PCR. The expression level was normalized to *Gapdh*. He, heart; Ki, kidney; Lu, lung; Sp, spleen; Ut, uterus; Te, testis; Ov, ovary; Li, liver; Br, brain; Mu, muscle. (B) Mouse tissue lysates (20 μ g total proteins) were immunoblotted with anti-*Zbed3* and anti-GAPDH (a load control). ES, mouse embryonic stem cells; Ov-null, ovary of *Zbed3*-null mice. (C) Paraffin sections of normal mouse ovary at day 14 after birth were stained with anti-*Zbed3* antibody for detecting endogenous *Zbed3* (red) and with Hoechst 33342 for labeling DNA (blue). Scale bar, 100 μ m. (D) The expression of *Zbed3* in mouse oocytes, eggs, and early embryos was detected by qRT-PCR. The expression level at GV stage was set as 1.0. (E) Lysates of oocytes, eggs, and early embryos were immunoblotted with anti-*Zbed3* antibody to detect endogenous *Zbed3*. GAPDH was the load control. Mo, morula; Bl, blastocyst. (F) Preimplantation embryos were stained with anti-*Zbed3* antibody to detect endogenous *Zbed3* (green) and with phalloidin to label F-actin (red). Scale bar, 20 μ m.

F-actin during the zygotic division progress (Figure 4A). After nuclear envelope breakdown (NEBD), microfilaments underwent dramatic remodeling, and a cloud of F-actin was formed around spindle in control zygotes at metaphase, which is consistent with previous reports (Chew et al., 2012; Yu et al., 2014). However, in zygotes from *Zbed3*^{Δ/Δ} females at the same stage (36/36), F-actin cloud around the spindle was disorganized after NEBD (Figure 4A). Furthermore, the bulk cytoplasmic F-actin in the zygotes from *Zbed3*^{Δ/Δ} females was loosened, rough and formed long fibers, while the controls exhibited dense F-actin structure (Figure 4B). The presence of disordered microfilaments was confirmed by microinjection of *GFP-Utrch* mRNA, an F-actin probe, into the live zygotes (Figure 4C). In addition, the cortical

F-actin in the zygotes from *Zbed3*^{Δ/Δ} females was thinner than that in controls (Figure 4D). These results suggest that the deficiency of maternal *Zbed3* impairs the F-actin network, resulting in off-center spindles in mouse zygotes.

Disordered F-actin cloud and cytoplasmic F-actin were also observed in *Zbed3*-null oocytes (Figure 4E). In maternal *Tle6*-null zygotes, the cloud of F-actin is disappeared because of decreased dephosphorylation (active form) of Cofilin, a depolymerizing factor for the microfilaments (Yu et al., 2014). However, immunoblots showed that the level of phosphorylated Cofilin S3 in maternal *Zbed3*-null zygotes was similar to that in the controls (Supplementary Figure S4), suggesting that *Zbed3* may regulate the formation of F-actin cloud via a different pathway.

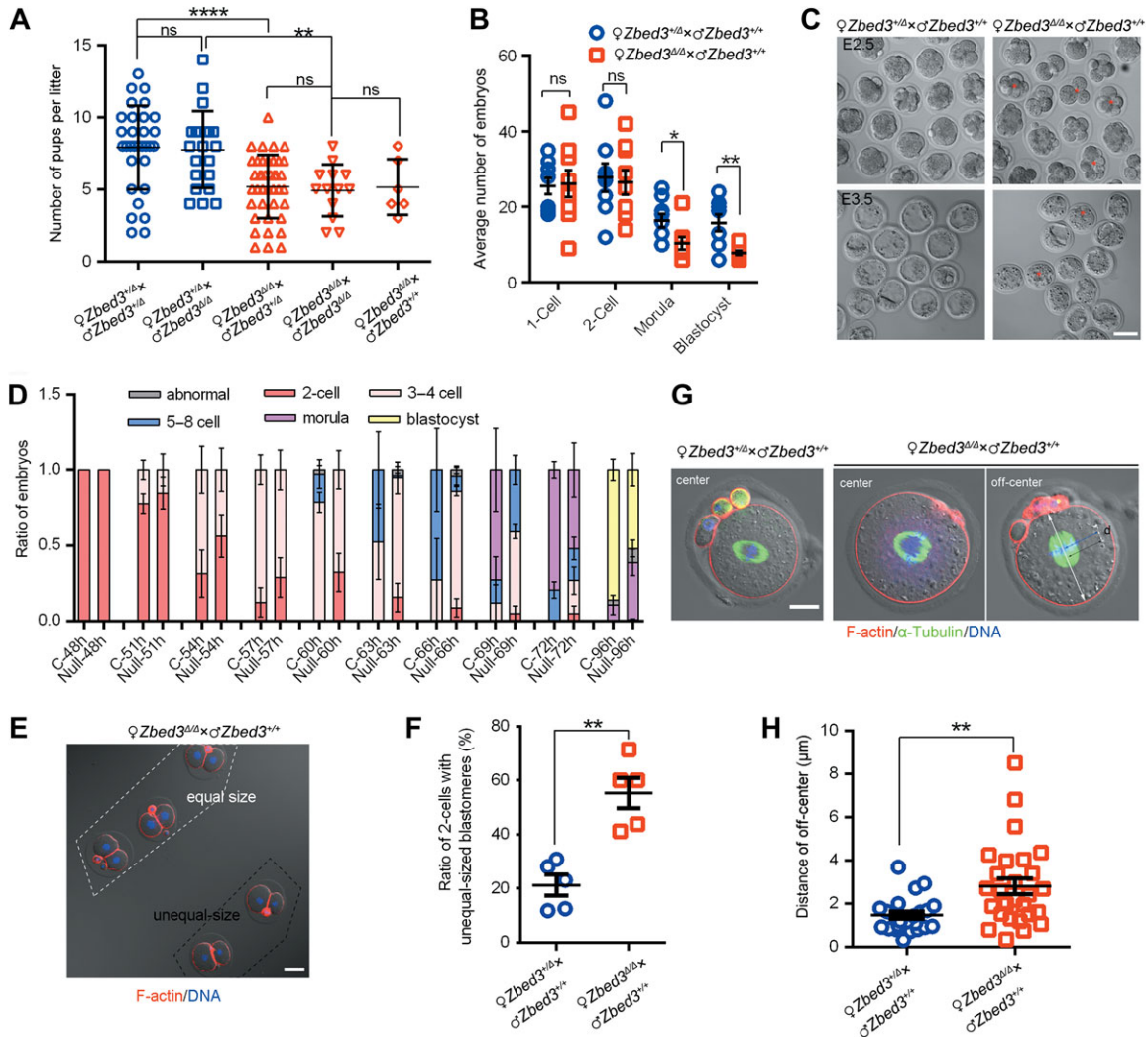


Figure 3 Maternal *Zbed3* deficiency affects normal development of early embryos. **(A)** After mating females with the males of various genotypes, litter sizes were calculated and presented as mean ± SEM. *****P* < 0.0001, ***P* = 0.0019. **(B)** Embryos at E0.5, 1.5, 2.5, 3.5 were isolated from *Zbed3*^{+/Δ} and *Zbed3*^{Δ/Δ} mice mated with wild-type (wt) males. Data were presented as mean ± SEM. ns, no significant. **P* = 0.0302, ***P* = 0.0037. **(C)** Light field images showing the morphology of morula (>8 cell, E2.5) and blastocyst (E3.5). Red * indicates impaired development of embryos. Scale bar, 50 μm. **(D)** 2-cell embryos (48 h after hCG) isolated from *Zbed3*^{+/Δ} (C, control) and *Zbed3*^{Δ/Δ} (Null, maternal null) females mated with wt males were cultured to blastocysts and the ratios of embryos at different stages (every 3 h) were calculated. The embryos were classified into 3–4 cell, 5–8 cell, >8 cell (morula), and blastocyst. **(E)** A representative image of 2-cell embryos from *Zbed3*^{Δ/Δ} females mated with wt males. These embryos were divided into two groups: with equal-sized blastomeres (in white dotted bordered rectangle) and with unequal-sized blastomeres (in black dotted bordered rectangle). Scale bar, 50 μm. **(F)** Ratios of 2-cell embryos with unequal-sized blastomeres were calculated in *Zbed3*^{+/Δ} and *Zbed3*^{Δ/Δ} females mated with wt males. Data were presented as mean ± SEM. ***P* = 0.0011. **(G and H)** The distance between the chromosome and cell center along the spindle long axis was shown in **G** and measured in **H**. Scale bar, 20 μm. Data were presented as mean ± SEM. ***P* = 0.0028.

Maternal *Zbed3* is required for the distributions of ER and mitochondria in zygotes and oocytes

During meiosis, FMN2-decorated endoplasmic reticulum (ER) polymerizes the cloud of F-actin following germinal vesicle breakdown (GVBD) of mouse oocyte (Yi et al., 2013). To examine whether the collapse of the F-actin cloud in zygotes from *Zbed3*^{Δ/Δ} females was caused by disruption of the FMN2-decorated ER, we injected zygotes with *GFP-Fmn2* mRNA and co-stained them with ER-Tracker. At metaphase, normal zygotes

formed a cloud of GFP-FMN2 that co-localized with ER around the spindle (8/8). However, FMN2-decorated ER was absent in the spindle periphery of maternal *Zbed3*-null zygotes (13/13) (Figure 5A). When treated with nocodazole to inhibit microtubules, normal zygotes failed to develop further due to the disintegrated spindles and the condensation of chromosomes, and exhibited the disorganized ER (Supplementary Figure S5A–C). In those zygotes, disordered F-actin clouds were observed, supporting the hypothesis that the disorganization of organelle

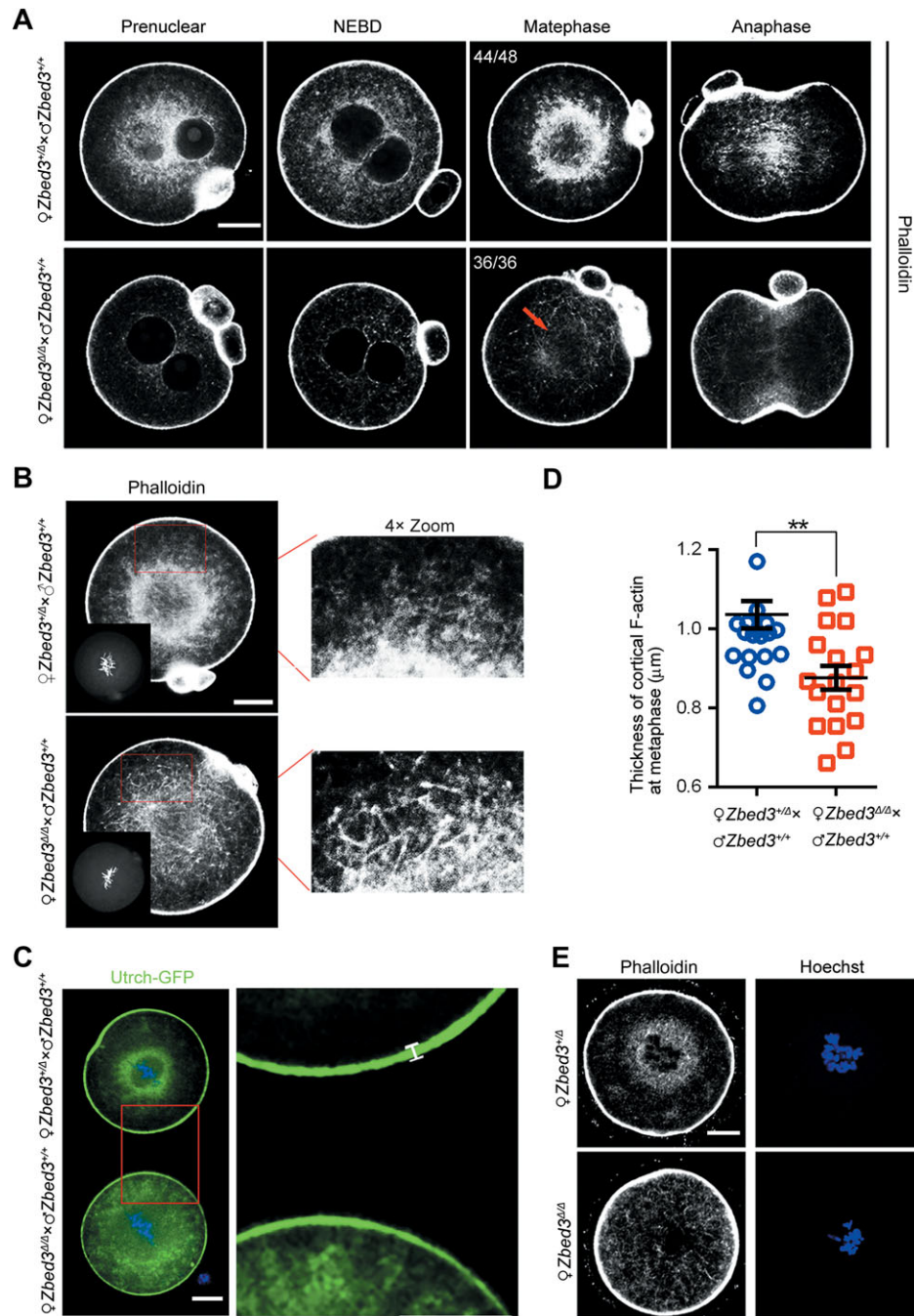


Figure 4 Disruption of maternal *Zbed3* impairs F-actin in mouse zygotes. **(A)** F-actin was stained with Alexa Fluor 488 Phalloidin at different stages of mitotic zygotes from *Zbed3*^{Δ/Δ} and *Zbed3*^{+/Δ} females mated with wt males. The red arrow indicates the residual and broken cloud of F-actin around spindle. **(B)** Cytoplasmic microfilaments (in red box) in zygotes from *Zbed3*^{Δ/Δ} and *Zbed3*^{+/Δ} females mated with wt males were compared at the similar stage of mitosis. **(C)** *GFP-Utrch* mRNA was microinjected into zygotes from *Zbed3*^{Δ/Δ} and *Zbed3*^{+/Δ} females mated with wt males to probe F-actin for live imaging. Chromosomes (blue) were marked with H2B-Tomato. **(D)** The thickness of cortical F-actin in **C** was measured. Data were presented as mean ± SEM. ***P* = 0.0015. **(E)** Oocytes from *Zbed3*^{Δ/Δ} and *Zbed3*^{+/Δ} females were cultured to GVBD, fixed, and stained with Phalloidin and Hoechst 33342 for labeling F-actin and DNA, respectively. Scale bar, 20 μm.

distribution results in disordered F-actin (Supplementary Figure S5A–C). These results indicated that the disorder of the F-actin cloud is caused by the misdistribution of FMN2-decorated ER in maternal *Zbed3*-null early embryos.

Because the ER generally couples with mitochondria during the remodeling of mouse oocytes (Dalton and Carroll, 2013), we tracked mitochondria using Mito-Tracker during mitosis of mouse zygotes. In control zygotes (9/9) from *Zbed3*^{+/Δ} females,

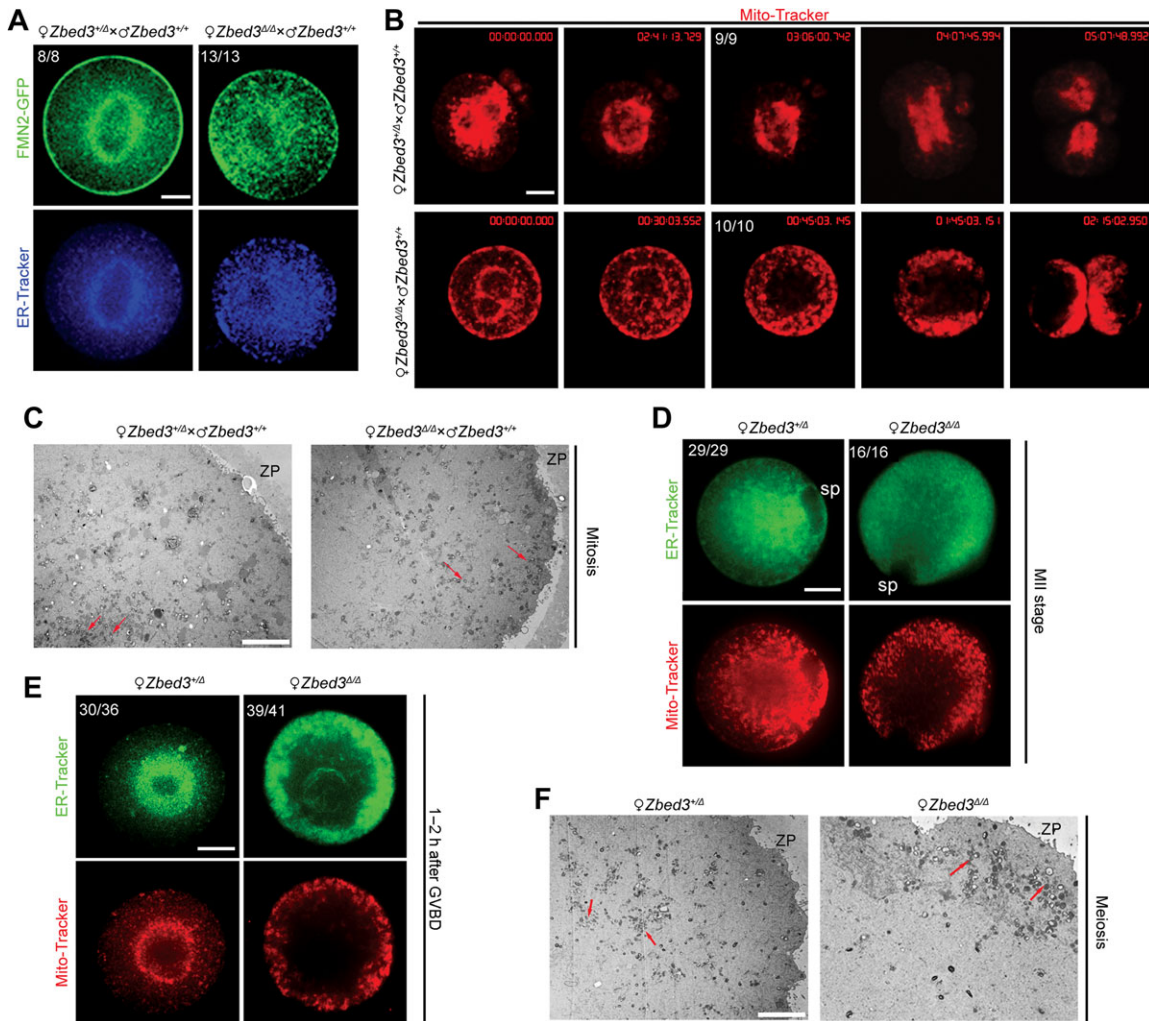


Figure 5 *Zbed3* deficiency impairs distribution of organelles. (A) Zygotes at metaphase from *Zbed3*^{Δ/Δ} and *Zbed3*^{+Δ} females mated with wt males were microinjected with *GFP-FMN2* mRNA and labeled with ER-Tracker (blue), and then imaged. Scale bar, 20 μm. (B) Distributions of mitochondria in the mitotic zygotes from *Zbed3*^{Δ/Δ} and *Zbed3*^{+Δ} females mated with wt males were tracked by Mito-Tracker for live imaging. Scale bar, 20 μm. (C) Mitochondria (red arrows) at zygotic metaphase were observed via TEM. Scale bar, 5 μm. (D and E) Oocytes at MII (D) and meiosis (E) stages from *Zbed3*^{Δ/Δ} and *Zbed3*^{+Δ} females were labeled with ER-Tracker (green) and Mito-Tracker (red) for living image. sp, spindle. Scale bar, 20 μm. (F) After GVBD, oocytes from *Zbed3*^{Δ/Δ} and *Zbed3*^{+Δ} females were fixed. TEM was used to observe the distribution of mitochondria (red arrows). ZP, zona pellucida. Red arrows point to the clusters of organelles. Scale bar, 5 μm.

the distribution of mitochondria was similar to that of ER (Figure 5B). In zygotes from *Zbed3*^{Δ/Δ} females (10/10), mitochondria were also located in both subcortical and perinuclear regions before NEBD. However, they accumulated at the subcortical region, resulting in the formation of a mitochondria-free zone in the center of the zygotes rather than forming a cloud-like structure around spindle after NEBD (Figure 5B). Using transmission electron microscopy (TEM), we found that mitochondria were mainly concentrated in the central areas of normal zygotes (3/3) at the mitotic stage. Mitochondria in the zygotes (3/3) from *Zbed3*^{Δ/Δ} females at similar stages were diffused in the cytoplasm and the subcortex (Figure 5C). These results indicate that *Zbed3* maintains the proper distribution of organelles during mitosis in mouse zygotes.

To investigate organelle distribution in the oocytes of *Zbed3*^{Δ/Δ} females, oocytes at MII stage from controls and *Zbed3*^{Δ/Δ} females were labeled with ER-Tracker and Mito-Tracker (Figure 5D). In control eggs (28/29), both organelles exhibited similar distributions: spreading from the spindle periphery to the cell center, and disappearing at the contralateral vegetal pole. However, in *Zbed3*^{Δ/Δ} eggs (16/16), the organelles were concentrated in the subcortex.

We then examined organelle distribution during meiosis by culturing mouse oocytes *in vitro* (Figure 5E). In 80.3% (30/36) of normal oocytes, the ER and mitochondria were distributed around the early spindle 1–2 h after GVBD. However, most *Zbed3*^{Δ/Δ} oocytes exhibited a subcortical plaque-like accumulation of both organelles (39/41), and a large organelle-free area

around the spindle in the cytoplasm (41/41). The TEM results confirmed the distribution of organelles in the oocytes from *Zbed3*^{Δ/Δ} females (3/3) (Figure 5F). These data indicated that Zbed3 is necessary for the normal redistribution of organelles during maturation of oocytes.

Zbed3 depends on, but is not required for, the formation of the SCMC

Disruption of core components results in the loss of the SCMC (Li et al., 2008b; Yu et al., 2014). Therefore, we examined Zbed3 in oocytes with disrupted core components of the SCMC. Compared to the controls, the level of Zbed3 was significantly decreased in *Tle6*, *Mater* or *Floped*-null oocytes at GV stages, while Zbed3 did not significantly change in *Filia*-null oocytes

(Figure 6A and B). Immunofluorescence staining showed that Zbed3 was less abundant in the cytoplasm of *Tle6* or *Mater*-null MII eggs than in normal and *Filia*-null oocytes, in which Zbed3 was still localized in the cytoplasm and subcortex (Figure 6C). These results revealed that the stability and localization of Zbed3 depend on the SCMC in mouse oocytes.

We then examined the formation of the SCMC in *Zbed3*-null oocytes. Immunoblots showed that the levels of SCMC core proteins were similar in the controls and *Zbed3*-null oocytes (Figure 6D). Immunofluorescence staining showed that the localizations of SCMC core proteins were similar to those of the controls (Figure 6E). Furthermore, co-IP experiments showed that the interactions between the SCMC proteins were not significantly affected in *Zbed3*^{Δ/Δ} oocytes (Figure 6F). Thus, Zbed3 is not required for formation of the SCMC.

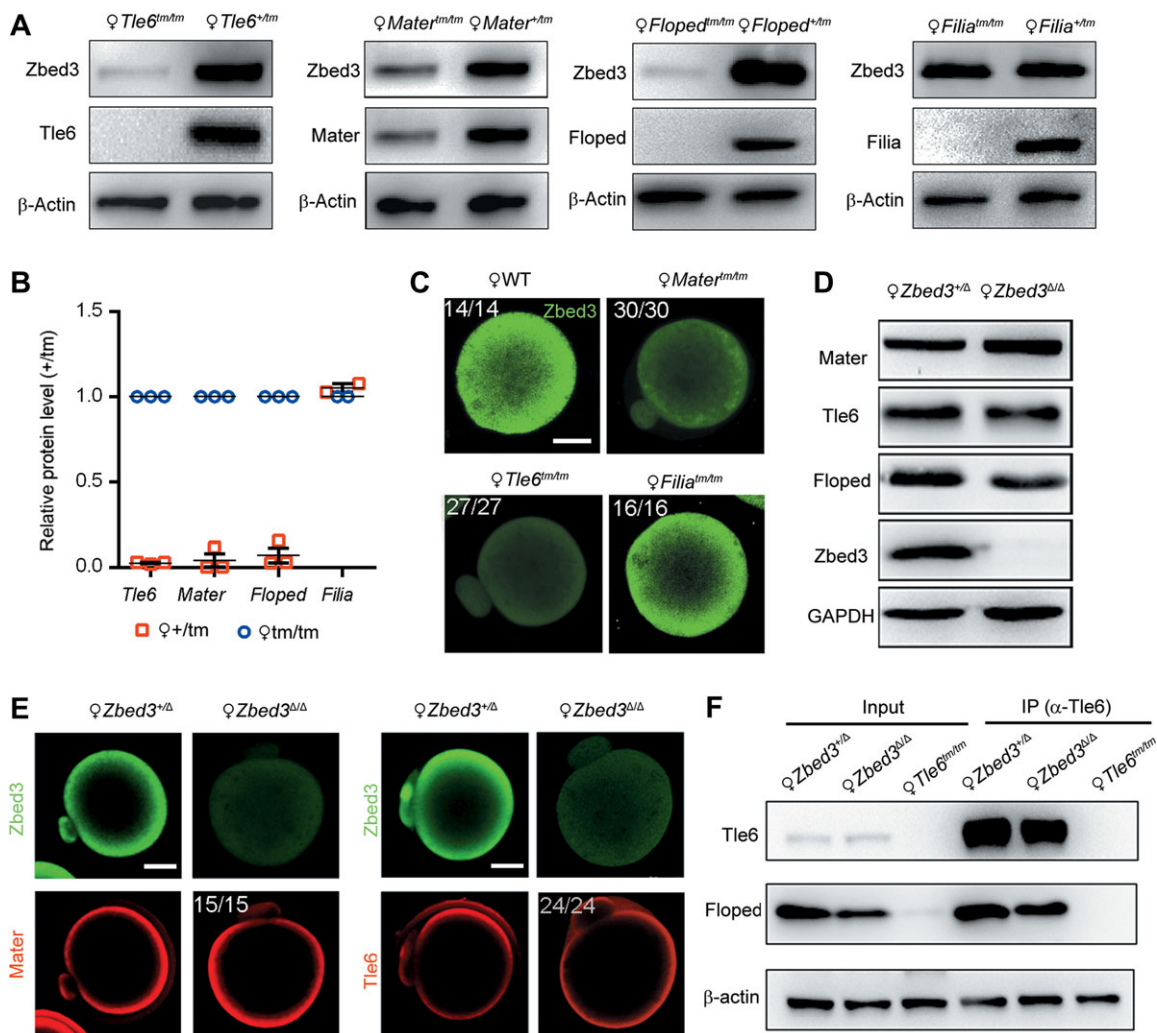


Figure 6 Zbed3 depends on, but is not required for, the formation of the SCMC. (A) Protein levels of Zbed3 were detected by immunoblots with mouse oocytes from females with a disrupted SCMC. β -actin was the load control. (B) Quantification of the protein levels of Zbed3 in A. The values in heterozygous oocytes were defined as 100%. (C) Oocytes from females with a disrupted SCMC were stained with anti-Zbed3 antibody (green). Scale bar, 20 μ m. (D) The levels of SCMC proteins in *Zbed3*^{+/ Δ} and *Zbed3* ^{Δ / Δ} oocytes were detected. GAPDH was the load control. (E) The SCMC core components were labeled in *Zbed3*^{+/ Δ} and *Zbed3* ^{Δ / Δ} oocytes. Scale bar, 20 μ m. (F) The interactions among the core components were detected by co-IP of ovarian lysates from *Zbed3*-null and *Tle6* mutant females.

Zbed3, as a downstream protein of the SCMC, regulates the distribution of ER and mitochondria via microtubules

Zbed3 depends on, but is not required for the formation of the SCMC, which suggests that Zbed3 might function as a downstream protein of the SCMC. To test this hypothesis, we examined the distribution of ER and mitochondria in oocytes and zygotes after disruption of the genes encoding SCMC core proteins. Zygotes and oocytes from *Tle6^{tm/tm}* and *Mater^{tm/tm}* females had similar defects with those from *Zbed3^{Δ/Δ}* females (Figure 7A and B). These results suggested that the impaired distributions of ER and mitochondria in maternal SCMC-null oocytes and zygotes may result from the loss of Zbed3.

The inhibition of microtubule dynamics using pharmacological reagents impacted the normal cloud of ER and mitochondria around the spindle in normal mouse oocytes (Supplementary Figure S5). We then examined whether the assembly of microtubules was normal after GVDB, when disordered distributions of ER and mitochondria were observed in oocytes with disrupted Zbed3. In the controls, a ball of microtubules was present around the chromosomes following microtubule organizing center congressing, consistent with previous report (Schuh and Ellenberg, 2007). In normal oocytes, the α -Tubulin pool in cytoplasm exhibited the decreased α -Tubulin signals at the spindle periphery where the extending astral-like microtubules of spindle were terminated. However, in *Zbed3^{Δ/Δ}* and *Tle6^{tm/tm}* oocytes, the α -Tubulin pool in cytoplasm was significantly extended in the subcortical region where elongated astral-like microtubules were terminated, rather than at spindle periphery (Figure 7C). The extent of extending α -Tubulin pool in the oocytes was calculated by the ratio of its area to that of the whole cell. Our results showed that the ratio in oocytes with disrupted Zbed3 (0.628 ± 0.036 , $n = 10$ oocytes) or *Tle6* (0.434 ± 0.027 , $n = 18$) was much larger than that in the controls (0.163 ± 0.022 , $n = 10$) (Figure 7D). By staining oocytes with MitoTracker and α -Tubulin-FITC, we observed that the subcortex of decreased α -Tubulin signals was the main location of mitochondria in oocytes with disrupted Zbed3. The plus-ends of elongated microtubules were observed to be co-localized with the subcortical mitochondria (Figure 7E). These results implied that deficiency of Zbed3 or the SCMC might exclude organelles to subcortex by affecting the dynamics of microtubules in cytoplasm and spindle of mouse oocytes. In addition, acetyl- α -Tubulin, a marker of microtubule dynamics and stability, was significantly decreased in oocytes from *Tle6^{tm/tm}* and *Zbed3^{Δ/Δ}* females (Figure 7F). Altogether, our data indicate that the SCMC or Zbed3 control the distributions of ER and mitochondria by regulating the cytoskeletal dynamics in mouse oocytes.

Zbed3 is involved in the formation of CPLs in mouse oocytes

Similar to Mater and Padi6 (Yurttas et al., 2008; Kim et al., 2010), Zbed3 was resistant to extraction with Triton X-100 (Figure 8A and B). After extraction, Zbed3 was partially co-localized with Mater in mouse oocytes (Figure 8C). Mater and Floped, two SCMC core proteins, have been shown to regulate the formation of CPLs, oocyte specific fibrous structure that is

essential for microtubules and organelle distributions (Kan et al., 2011; Kim et al., 2014). Using TEM, we observed the disappearance of CPLs in *Zbed3*-null oocytes (Figure 8D).

In addition, we found that the distribution of CPLs was non-uniform in normal mouse oocyte cytoplasm: the area with the fewest organelles had the most CPLs (Figure 8E and F). Immunofluorescent staining of Zbed3 and mitochondria showed that mitochondria was not co-localized with, but nested in Zbed3 signals in cytoplasm of normal mouse oocytes, and the Zbed3 signal was very weak in the periphery of the spindle where organelles were abundant (Figure 8G). We also found that the cluster of organelles was embedded in the honeycomb-like CPLs, using TEM (Figure 8H). Altogether, these data suggest that Zbed3 is involved in CPL formation that may be related to the regulation of organelle distributions.

Discussion

The absence of a single core protein (Mater, Floped or *Tle6*) prevents the formation of the SCMC, and complicates investigations of the roles of individual proteins in mutant phenotypes (Li et al., 2008b; Yu et al., 2014). In this study, we identified Zbed3 as a novel component of the SCMC. Mutant *Zbed3* female mice exhibit a mild reproductive phenotype and provide an excellent model to define the specific roles of the SCMC in female reproduction. The major defects observed in SCMC-null mice are also present in *Zbed3*-null mice, and include: asymmetrically divided zygotes, off-centered metaphase spindles, misdistributions of the ER and mitochondria, disorganized microfilaments and microtubules and the disruption of CPL formation (Li et al., 2008b; Fernandes et al., 2012; Kim et al., 2014; Yu et al., 2014). Furthermore, Zbed3 depends on, but is not required for the formation of the SCMC, which indicates that the SCMC regulates the development of mouse oocytes and early embryos by stabilizing downstream Zbed3. Thus, our results suggest that Zbed3, as a downstream protein of SCMC, regulates the distribution of organelles through controlling cytoskeletal dynamics and/or CPL formation.

CPLs are fibrous structure restricted in mammalian oocytes and early embryos. However, the components, formation, and function of CPLs are still poorly understood since it was discovered (Hadek, 1966). Eptidylarginine deiminase 6 (Padi6) is located in CPLs and required for the formation of CPLs (Yurttas et al., 2008; Kan et al., 2011; Liu et al., 2017). The disruption of Padi6 leads to the absence of CPLs and the defects of organelle distributions, implying CPLs take a role in organelle distributions (Yurttas et al., 2008; Kan et al., 2011). Recently, increasing evidences have shown that both of the SCMC and CPLs are closely related (Kim et al., 2010, 2014; Tashiro et al., 2010; Monti et al., 2013). The SCMC proteins, Floped and Mater are also localized in the CPLs. Depletion of them results in the absence of CPLs in mouse oocytes (Kim et al., 2010; Tashiro et al., 2010). The abnormal redistribution of organelles was also observed in *Mater*-null oocytes (Kan et al., 2011; Fernandes et al., 2012; Kim et al., 2014). Here, we find that the absence of CPLs is correlated with the disorganized distributions of

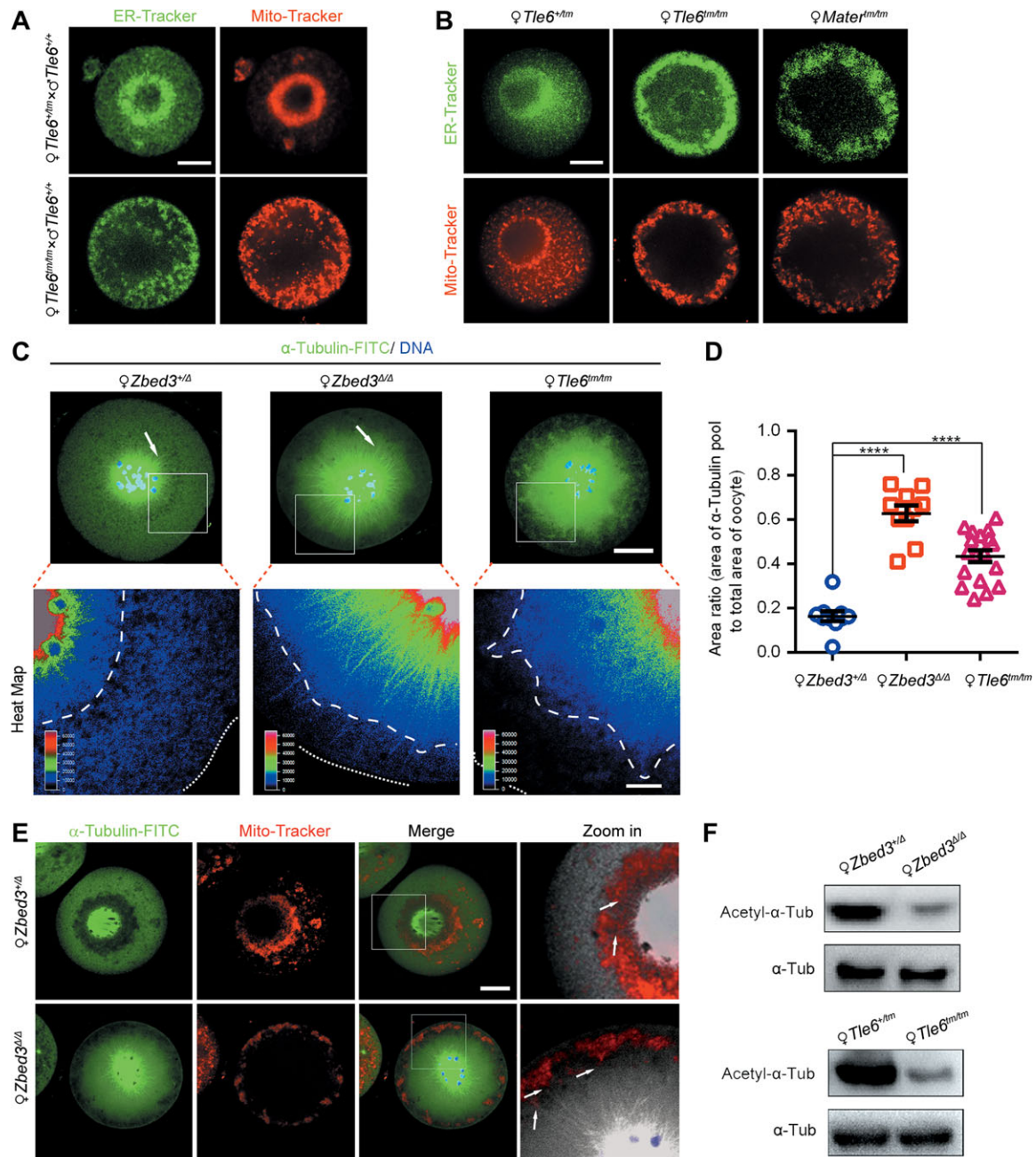


Figure 7 Zbed3 maintains proper dynamics of microtubules in oocytes. **(A and B)** ER and mitochondria were labeled with ER-Tracker (green) and Mito-Tracker (red) in zygotes or oocytes from *Tle6*^{tm/tm} or *Mater*^{tm/tm} females (mated with wt males for zygotes). Scale bar, 20 μm . **(C)** Microtubules were stained with anti- α -Tubulin-FITC in control, *Zbed3*-null, and *Tle6*-null oocytes. White arrows point to the astral-like microtubules from spindle in upper panels. Scale bar, 20 μm . Bottom panels are heat maps for white boxes in upper panels. The inner area of the dashed line was defined as α -Tubulin pool, and the dotted line was the outer edge of the cell. Scale bar, 5 μm . **(D)** The extent of extending α -Tubulin pool in **C** was measured by dividing the area of α -Tubulin pool by total cellular area in oocytes from control, *Zbed3*^{Δ/Δ}, or *Tle6*^{tm/tm} females. Data were presented as mean \pm SEM. *****P* < 0.0001. **(E)** Oocytes from *Zbed3*^{+/Δ} and *Zbed3*^{Δ/Δ} females were cultured to GVBD in medium with Mito-Tracker (red), fixed, and then stained with anti- α -Tubulin-FITC antibody (green). White arrows indicate potential interactions between mitochondria and the plus end of microtubules. Scale bar, 20 μm . **(F)** The acetyl α -Tubulin at Lys40 and α -Tubulin were detected by immunoblots with oocytes from *Zbed3*-null and *Tle6* mutant females.

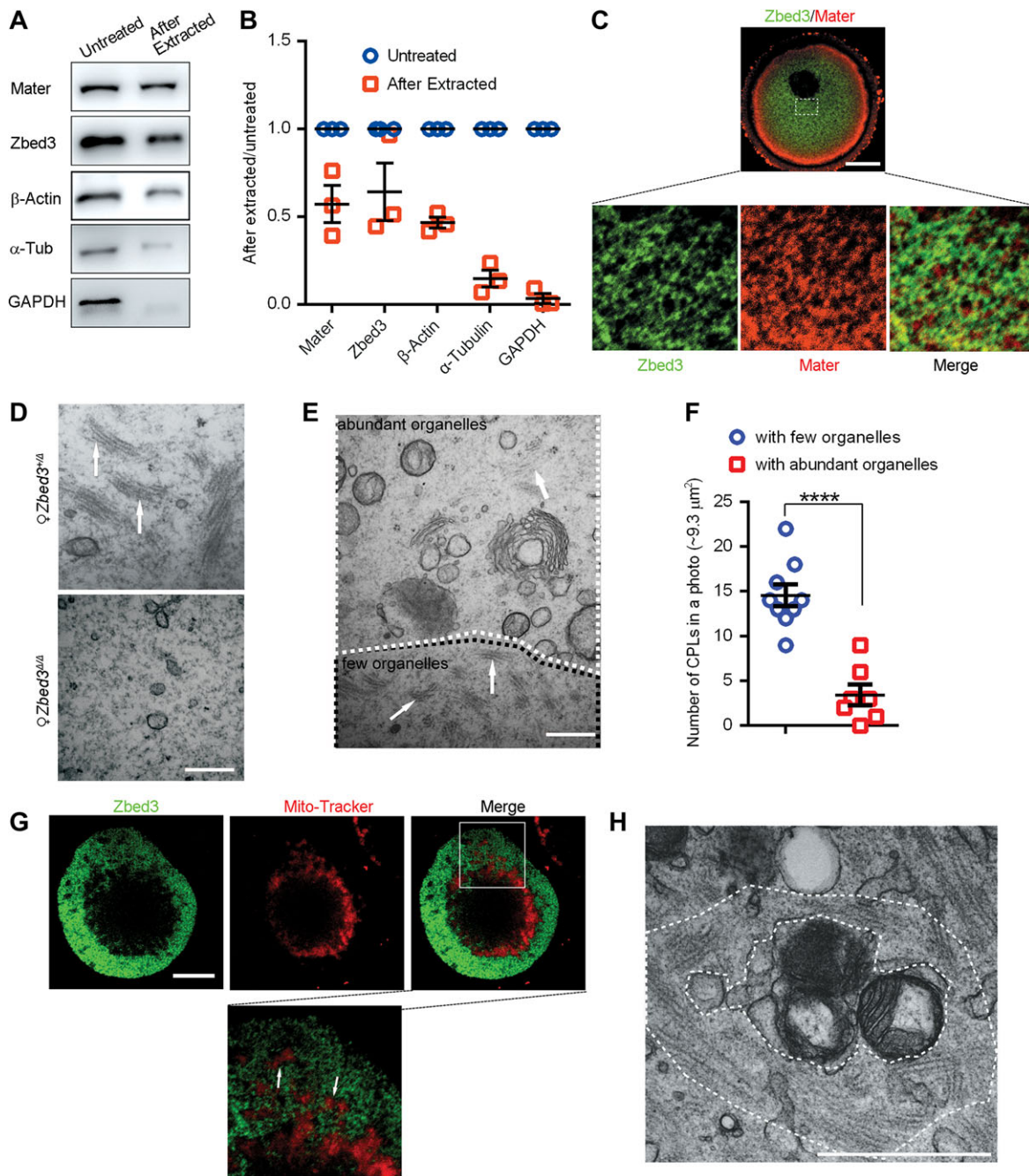


Figure 8 Zbed3 is involved in the formation of CPLs. **(A)** Normal oocytes extracted in a buffer with 1% Triton X-100 were immunoblotted. **(B)** The quantification of protein levels in **A**. The values in untreated oocytes were defined as 100%. **(C)** Oocytes were co-stained with anti-Zbed3 (green) and anti-Mater (red) antibodies. Scale bar, 20 μm (top) and 5 μm (bottom). **(D)** CPLs in oocytes from *Zbed3*^{+/Δ} and *Zbed3*^{ΔΔ} females were observed by TEM, respectively. White arrows point to CPLs. Scale bar, 500 nm. **(E)** Distributions of CPLs in the areas of few and abundant organelles were showed. The areas with few and abundant organelles were circumscribed with black and white dotted line. White arrows point to CPLs. Scale bar, 500 nm. **(F)** The number of CPLs was quantified. The pictures ($\sim 9.3 \mu\text{m}^2$) with few or abundant organelles were selected from 5 normal oocytes. Data were presented as mean \pm SEM. **** $P < 0.0001$. **(G)** Normal oocytes in meiosis were labeled with Mito-tracker (red), fixed, and then stained with anti-Zbed3 antibody (green). White arrows point to mitochondria. Scale bar, 20 μm . **(H)** Clusters of mitochondria and CPLs in wt oocyte were observed by TEM. Scale bar, 500 nm.

organelles in the *Zbed3*-null oocytes. Thus, these results suggest that Zbed3 or the SCMC regulates organelle distributions through CPLs.

How CPLs control the distribution of organelles is still unclear (Kan et al., 2011). In current study, we find that CPLs are not uniformly distributed in the cytoplasm of mouse oocytes. CPLs are rarely distributed in the areas of abundant organelles, and typically enriched in organelle-free regions (Figure 8E and F). Thus, CPLs might form a specific structure surrounding the organelles (Figure 8G and H), which suggests that the CPLs may function as a honeycomb-like or barrier structure to maintain the locations of single organelle or clusters of them in mouse oocytes. Consistent with this hypothesis, mitochondria in *Zbed3*-null oocytes are observed to be accumulated as plaque-like structures (Figure 5E and F), similar to that around the spindle of normal oocytes (Figure 8G), in which the CPLs might be accompanied with the cytoskeleton and reorganized (Li et al., 2008a). The disappearance of CPLs may increase the probability of organelle accumulation and movement.

Studies have revealed that skeleton components, F-actin, microtubules, and intermediate filaments were detected in CPLs (McGaughey and Capco, 1989; Gallicano et al., 1994; Kan et al., 2011), implying CPLs may function coupling with the skeleton dynamics in several key developmental stages of oocyte and embryo (Jackson et al., 1980; McGaughey and Capco, 1989). During mitosis, the organelles are excluded from the spindle, which is required for assembly of chromosomes (Lu et al., 2009; Smyth et al., 2012; Schlaitz et al., 2013; Maddox and Ladouceur, 2015; Schweizer et al., 2015). The process is regulated by ER-related proteins (such as REEP3/4 and STIM1) and microtubule-related proteins (such as EB1) in a microtubule-dependent manner (Smyth et al., 2012; Schlaitz et al., 2013). We find that the microtubules extending from the spindle are always terminated at the edge of the organelle cloud in normal mouse oocyte, suggesting the organelles are excluded from the spindle in mouse oocytes. In oocytes with mutant *Zbed3* or disrupted the SCMC, excessively elongated microtubules and cytoplasmic α -Tubulin pool occupy greater area than in the control and exclude ER and mitochondria into the subcortex. In addition, the decreased acetyl- α -Tubulin suggests that cytoplasmic microtubules are unstable. Zbed3 has been reported to bind directly to Axin1, forming a complex with APC, a well-known regulator of microtubule plus-ends in somatic cells (Behrens et al., 1998; Farr et al., 2000; Chen et al., 2009; Preitner et al., 2014). Thus, the cytoplasmic distribution of Zbed3 may maintain the proper distribution of organelles in the cytoplasm by regulating the dynamics of CPLs or microtubules.

Although the maturation and fertilization of *Zbed3*-null oocytes are almost normal (Supplementary Figure S6), the CPLs, cytoskeleton, and distributions of the ER and mitochondria are disorganized. Furthermore, the ratio of 2-cell stage mutant embryos with unequally sized blastomeres is increased and fewer mutant embryos develop into blastocysts. These findings suggest that mouse oocytes and early embryos are tolerant to the defects in organelle distribution, CPLs, and cytoskeleton. The

adverse effects of disordered organelles, or impaired cytoskeletons and CPLs may not be sufficient to affect oocyte survival, ovulation, and fertilization. Accompanying the development, the damages might be accumulated and lead to delayed or impaired developmental potential in maternal *Zbed3*-null early embryos. Except for the arrested 2-cell embryo stage, most of phenotypes of *Zbed3* knockout mice were also observed in females with depletion of core SCMC components, implying that the SCMC or its core components may affect other factors that are essential for development beyond the 2-cell stage.

Materials and methods

Mouse maintenance, establishment of Zbed3 knockout mouse, and collection of oocytes and preimplantation embryos

All mouse lines were kept in compliance with the guidelines of the Animal Care and Use Committee of the Institute of Zoology at the Chinese Academy of Sciences. To establish *Zbed3* knockout mouse, the gene targeting vector from the International Mouse Phenotyping Consortium (IMPC) was linearized and electro-transformed into mice ES cells. After selection with G418, the positive clones were identified through long PCR amplification with specific primers (Supplementary Table S1, Figure S2A and B). To identify correct recombination, the products of long PCR amplification between homologous arms and the original genome or loxPs were sequenced. The targeted cells were microinjected into mouse blastocysts which were subsequently transplanted into surrogate mothers for birth. After germline transition, the heterozygous males and females were mated to obtain *Zbed3*^{F/F} mice. To delete exon 2 of *Zbed3*, *Zbed3*^{F/F} females were mated with *Zp3-Cre* males, and their offspring were termed *Zbed3*^{+/ Δ} . *Zbed3* mutant mice were genotyped using DNA of mouse tails as templates for PCR reaction with three oligo-primers, which produced the wild-type (+, 189 bp) and mutant alleles (Δ , 317 bp). The collection of mouse oocytes and preimplantation embryos was performed as described previously (Yu et al., 2014; Xu et al., 2015). To isolate oocytes, CD1 female mice (5–7 weeks old) were stimulated with PMSG (5 IU). After 46–48 h, ~80 μ m diameter oocytes at the GV stage were isolated from ovarian follicles. MII eggs were collected about 12–14 h after additional hCG (5 IU) stimulation. Preimplantation embryos at the zygote, 2-cell, morula, and blastocyst stages were recovered from the plugged females at 24, 48, 72, and 96 h after hCG stimulation, respectively.

Oocyte co-IP, silver staining, and mass spectrometry

For oocyte co-IP, ~3000 GV and MII eggs were lysed in lysis buffer (25 mM Tris, 150 mM NaCl, 1 mM EDTA, 1% NP-40, 5% glycerol, Roche 1 \times Complete Protease Inhibitor Cocktail, pH 7.4) on ice for 15–30 min. The lysates were centrifuged at 12000 rpm for 15 min at 4°C. The supernatants were cleared using 15 μ l agarose protein G beads (Santa Cruz, sc-2002) 4°C for 1 h. Mouse anti-Mater antibody, anti-Tle6 antibody (Yu et al., 2014), or IgG (1:100, Santa Cruz, sc-2025) was added, and the resulting mixtures were incubated at 4°C for 2 h. The mixtures were then incubated with 15 μ l agarose protein G

beads at 4°C overnight. After washing, the beads were re-suspended in 1× SDS loading buffer and incubated at 95°C for 5 min. The precipitates were separated in 10% SDS-PAGE gel. Because the infrequent distinct protein bands were distinguished after the gel was stained using the silver stain kit (Sigma, PROTSIL1), we removed the light and weight chains of IgG to prevent their interference and collected all proteins on the gels as a sample for mass spectrometry (NanoLC-LTQ-Orbitrap XL, Thermo Finnigan).

mRNA extraction and quantitative RT-PCR

mRNAs were extracted from oocytes, early embryos, and tissues using a Dynabeads mRNA Direct Micro Kit (Ambion, 61021), and dissolved in RNase-free water. Reverse transcription of mRNA was performed using PrimeScript RT Reagent Kit (Takara, RR037A). Quantitative RT-PCR was performed using EvaGreen qPCR MasterMix (Applied Biological Materials, MasterMix-LR) with primers of either *Zbed3* or *Gapdh* as a reference (Supplementary Table S1). The results were calculated on the basis of $2^{-\Delta\Delta Ct}$ values.

Protein–protein interactions in vitro

To examine protein–protein interactions *in vitro*, the CDSs of *Tle6*, *Floped*, *Mater*, and *Zbed3* were cloned into pCMV-HA and p3×FLAG-CMV10 expression vectors with specific primers (Supplementary Table S1). The recombinant plasmids were purified from *E.coli* using a TIANpure Midi Plasmid kit (TIANGEN, DP107-02), dissolved in double-distilled water and stored at –20°C. HEK-293T cells were cultured in DMEM (Gibco, C11995500BT) containing 10% fetal bovine serum at 37°C with 5% CO₂. Before transfection, the cells were plated in 60 mm dishes at 80%–90% confluence. Based on the manufacturer's instructions for Lipofectamine 2000 Transfection Reagent (Invitrogen, 11668-027), ~8 µg total vector (pCMV-HA-*Tle6*/*Mater*/*Floped*/*Filia*: 5 µg, p3×FLAG-CMV10-*Zbed3*: 3 µg) were co-transfected per dish. After 36 h, the transfected cells were harvested and lysed in 500 µl buffer (25 mM Tris, 150 mM NaCl, 1 mM EDTA, 1% NP-40, 5% glycerol, Roche 1× Complete Protease Inhibitor Cocktail, pH 7.4). Mouse anti-HA antibody (1:200, Abmart) was used for co-IP experiments as described above. Approximately 5% cell lysates were directly incubated at 95°C for 5 min as the input.

Oocyte and embryo vital staining

For organelles staining, oocytes or zygotes were cultured in M2 medium or KSOM medium with Mito-Tracker Red CMXRos (1:10000, Invitrogen, M7512) and ER-Tracker Blue-White DPX (1:5000, Invitrogen, E12353) for 1 h at 37°C, with 5% CO₂. To determine the effects of cytoskeletal disruption on organelle distribution in oocytes, nocodazole (1 µM, Sigma, m1404) or latrunculin A (1 µg/ml, Sigma, L5163) were added following GVBD. After incubation, oocytes or zygotes were washed and transferred to glass-bottom dishes. Live confocal microscopy

(Carl Zeiss, LSM510) was used to acquire digital images which were progressed further using Volocity 3D Image Analysis Software.

Immunoblots and immunofluorescent staining

The samples for immunoblots were separated by SDS-PAGE and transferred to PVDF membranes (Millipore, IPVH00010). The membranes were blocked in PBS/0.1% Tween-20 (PBST) with 5% milk for 1 h at RT. The membranes were then incubated with primary antibodies overnight at 4°C, washed three times with PBST, and incubated with HRP-conjugated secondary antibodies (1:5000, ZSGB-BIO) at RT for 1 h. Protein bands were detected by immune-reactivity using a ChemiDoc XRS+ System (Bio-Rad) and the resulting images were edited using Quantity One software (Bio-Rad).

Immunofluorescence staining was conducted using a modified version of our previously reported protocol (Yu et al., 2014). For F-actin or α-Tubulin staining, oocytes or zygotes (*in vitro*: cultured; *in vivo*: directly recovered) were fixed in buffer (130 mM KCl, 25 mM HEPES pH 7.0, 3 mM MgCl₂, 4% paraformaldehyde, 0.15% glutaraldehyde, 0.2% Triton X-100) for >2 h at RT, permeabilized in PBS with 0.5% Triton X-100 for 30 min, blocked with 1% BSA at RT for 1 h, and incubated with Alexa Fluor 488 Phalloidin or 546 Phalloidin (1:200, Invitrogen), or mouse anti-α-Tubulin antibody conjugated with FITC (1:200, Sigma) for 2 h at RT. For staining of other proteins, the samples were fixed with 4% PFA in PBS, and incubated with primary antibodies for 1.5–2 h at RT, and with secondary antibodies (1:200, Invitrogen) at RT for 1 h. Images were acquired using an LSM 780 confocal microscope and processed using ZEN 2012 software. The comparative fluorescence intensities were imaged under the same laser power.

The primary antibodies used in our experiments are listed in Supplementary Table S2.

Transmission electron microscopy

About 15 oocytes (1–2 h after GVBD) and zygotes at metaphase (1 h after NEBD) were fixed in 0.1 M Na-cacodylate with 4% PFA and 2.5% glutaraldehyde for 2 h at RT, embedded in 4% agar, and stored in the fixation buffer. The samples were sent to the electron microscope facility at China Agricultural University for processing. After dehydration through an alcohol gradient, the samples were embedded in LX112 resin and sectioned. The resulting grids were observed by TEM (Jeol, JEM-1230).

Microinjection experiment

Microinjection was performed as described previously (Yu et al., 2014). Briefly, the CDS of genes were cloned into pCS2-6×Myc vector. The mRNAs were transcribed from linearized vectors using a mMESAGE mMACHINE Kit (Ambion, AM1340) according to the manufacturer's instructions. Oocytes or zygotes were injected using micromanipulator system (Nikon), and then cultured until specific time points.

Extraction of oocytes

The extraction protocols were conducted using a modified version of previously reported protocol (Capco et al., 1993). Mouse oocytes were extracted in a buffer (100 mM NaCl, 3 mM MgCl₂, 10 mM EGTA, 10 mM HEPES, 1% Titron X-100 and Complete Protease Inhibitor Cocktail, pH 7.5) for 20 min, and then washed three times with 0.1% BSA/PBS. Oocytes were collected for immunofluorescence staining or western blotting.

Statistical analysis

Quantitative analyses were performed based on at least three independent biological samples. Data were represented as mean ± SEM. GraphPad Prism software was used to conduct Student's *t*-tests to determine the statistical significance of differences between two groups exhibiting Gaussian distributions. *P* < 0.05 was considered to indicate statistical significance.

Supplementary material

Supplementary material is available at *Journal of Molecular Cell Biology* online.

Acknowledgements

We thank Lijuan Wang, Shiwen Li, and Xili Zhu (Institute of Zoology, Chinese Academy of Science) for technical assistance and Dr Jurrien Dean at National Institutes of Health in USA for critical review of the manuscript.

Funding

This work was funded by the National Natural Science Foundation of China (31471353, 31590832) and the Strategic Priority Research Program of the Chinese Academy of Sciences (XDA01010103).

Conflict of interest: none declared.

Author contributions: Z.G. designed and performed major experiments, analyzed the data, and wrote the manuscript. X.Z. established the *Zbed3*-null transgenic mouse line and obtained the electron microscopy data. X.Y., D.Q., Y.X., Y.Y., Yu.X., X.N., X.L., and W.L. contributed to mouse maintenance, F-actin experiments, oocyte and embryo isolation. Z.Y. analyzed the data. L.L. initiated and organized the study, analyzed the data, and wrote the manuscript. All authors commented on the manuscript.

References

- Alazami, A.M., Awad, S.M., Coskun, S., et al. (2015). TLE6 mutation causes the earliest known human embryonic lethality. *Genome Biol.* **16**, 240.
- Bebbere, D., Ariu, F., Bogliolo, L., et al. (2014). Expression of maternally derived KHDC3, NLRP5, OOEP and TLE6 is associated with oocyte developmental competence in the ovine species. *BMC Dev. Biol.* **14**, 40.
- Bebbere, D., Masala, L., Albertini, D.F., et al. (2016). The subcortical maternal complex: multiple functions for one biological structure? *J. Assist. Reprod. Genet.* **33**, 1431–1438.
- Behrens, J., Jerchow, B.A., Wurtele, M., et al. (1998). Functional interaction of an axin homolog, conductin, with β -catenin, APC, and GSK3 β . *Science* **280**, 596–599.
- Capco, D.G., Gallicano, G.I., McGaughey, R.W., et al. (1993). Cytoskeletal sheets of mammalian eggs and embryos: a lattice-like network of intermediate filaments. *Cell Motil. Cytoskeleton* **24**, 85–99.
- Chaigne, A., Campillo, C., Voituriez, R., et al. (2016). F-actin mechanics control spindle centring in the mouse zygote. *Nat. Commun.* **7**, 10253.
- Chen, T., Li, M., Ding, Y., et al. (2009). Identification of zinc-finger BED domain-containing 3 (*Zbed3*) as a novel Axin-interacting protein that activates Wnt/ β -catenin signaling. *J. Biol. Chem.* **284**, 6683–6689.
- Chew, T.G., Lorthongpanich, C., Ang, W.X., et al. (2012). Symmetric cell division of the mouse zygote requires an actin network. *Cytoskeleton* **69**, 1040–1046.
- Dalton, C.M., and Carroll, J. (2013). Biased inheritance of mitochondria during asymmetric cell division in the mouse oocyte. *J. Cell Sci.* **126**, 2955–2964.
- Docherty, L.E., Rezwan, F.I., Poole, R.L., et al. (2015). Mutations in NLRP5 are associated with reproductive wastage and multilocus imprinting disorders in humans. *Nat. Commun.* **6**, 8086.
- Farr, G.H., Ferkey, D.M., Yost, C., et al. (2000). Interaction among GSK-3, GBP, axin, and APC in *Xenopus* axis specification. *J. Cell Biol.* **148**, 691–702.
- Fernandes, R., Tsuda, C., Perumalsamy, A.L., et al. (2012). NLRP5 mediates mitochondrial function in mouse oocytes and embryos. *Biol. Reprod.* **86**, 138, 131–110.
- Gallicano, G.I., Larabell, C.A., McGaughey, R.W., et al. (1994). Novel cytoskeletal elements in mammalian eggs are composed of a unique arrangement of intermediate filaments. *Mech. Dev.* **45**, 211–226.
- Gu, T.P., Guo, F., Yang, H., et al. (2011). The role of Tet3 DNA dioxygenase in epigenetic reprogramming by oocytes. *Nature* **477**, 606–610.
- Hadek, R. (1966). Cytoplasmic whorls in the golden hamster oocyte. *J. Cell Sci.* **1**, 281–282.
- Hayward, A., Ghazal, A., Andersson, G., et al. (2013). ZBED evolution: repeated utilization of DNA transposons as regulators of diverse host functions. *PLoS One* **8**, e59940.
- Herr, J.C., Chertihin, O., Digilio, L., et al. (2008). Distribution of RNA binding protein MOEP19 in the oocyte cortex and early embryo indicates pre-patterning related to blastomere polarity and trophectoderm specification. *Dev. Biol.* **314**, 300–316.
- Jackson, B.W., Grund, C., Schmid, E., et al. (1980). Formation of cytoskeletal elements during mouse embryogenesis. Intermediate filaments of the cyokeratin type and desmosomes in preimplantation embryos. *Differentiation* **17**, 161–179.
- Kan, R., Yurttas, P., Kim, B., et al. (2011). Regulation of mouse oocyte microtubule and organelle dynamics by PADI6 and the cytoplasmic lattices. *Dev. Biol.* **350**, 311–322.
- Kim, B., Kan, R., Anguish, L., et al. (2010). Potential role for MATER in cytoplasmic lattice formation in murine oocytes. *PLoS One* **5**, e12587.
- Kim, B., Zhang, X., Kan, R., et al. (2014). The role of MATER in endoplasmic reticulum distribution and calcium homeostasis in mouse oocytes. *Dev. Biol.* **386**, 331–339.
- Li, H., Guo, F., Rubinstein, B., et al. (2008a). Actin-driven chromosomal motility leads to symmetry breaking in mammalian meiotic oocytes. *Nat. Cell Biol.* **10**, 1301–1308.
- Li, L., Baibakov, B., and Dean, J. (2008b). A subcortical maternal complex essential for preimplantation mouse embryogenesis. *Dev. Cell* **15**, 416–425.
- Li, L., Lu, X., and Dean, J. (2013). The maternal to zygotic transition in mammals. *Mol. Aspects Med.* **34**, 919–938.
- Li, L., Zheng, P., and Dean, J. (2010). Maternal control of early mouse development. *Development* **137**, 859–870.
- Li, R., and Albertini, D.F. (2013). The road to maturation: somatic cell interaction and self-organization of the mammalian oocyte. *Nat. Rev. Mol. Cell Biol.* **14**, 141–152.
- Lin, C.J., Koh, F.M., Wong, P., et al. (2014). Hira-mediated H3.3 incorporation is required for DNA replication and ribosomal RNA transcription in the mouse zygote. *Dev. Cell* **30**, 268–279.
- Liu, X., Morency, E., Li, T., et al. (2017). Role for PADI6 in securing the mRNA-MSY2 complex to the oocyte cytoplasmic lattices. *Cell Cycle* **16**, 360–366.

- Liu, Y., Lu, X., Shi, J., et al. (2016). BTG4 is a key regulator for maternal mRNA clearance during mouse early embryogenesis. *J. Mol. Cell Biol.* *8*, 366–368.
- Lu, L., Ladinsky, M.S., and Kirchhausen, T. (2009). Cisternal organization of the endoplasmic reticulum during mitosis. *Mol. Biol. Cell* *20*, 3471–3480.
- Maddox, P.S., and Ladouceur, A.M. (2015). Concentrating on the mitotic spindle. *J. Cell Biol.* *210*, 691–693.
- McGaughey, R.W., and Capco, D.G. (1989). Specialized cytoskeletal elements in mammalian eggs: structural and biochemical evidence for their composition. *Cell Motil. Cytoskeleton* *13*, 104–111.
- Monti, M., Zanoni, M., Calligaro, A., et al. (2013). Developmental arrest and mouse antral not-surrounded nucleolus oocytes. *Biol. Reprod.* *88*, 2.
- Ohsugi, M., Zheng, P., Baibakov, B., et al. (2008). Maternally derived FLI1-MATER complex localizes asymmetrically in cleavage-stage mouse embryos. *Development* *135*, 259–269.
- Parry, D.A., Logan, C.V., Hayward, B.E., et al. (2011). Mutations causing familial biparental hydatidiform mole implicate c6orf221 as a possible regulator of genomic imprinting in the human oocyte. *Am. J. Hum. Genet.* *89*, 451–458.
- Preitner, N., Quan, J., Nowakowski, D.W., et al. (2014). APC is an RNA-binding protein, and its interactome provides a link to neural development and microtubule assembly. *Cell* *158*, 368–382.
- Schlaitz, A.L., Thompson, J., Wong, C.C., et al. (2013). REEP3/4 ensure endoplasmic reticulum clearance from metaphase chromatin and proper nuclear envelope architecture. *Dev. Cell* *26*, 315–323.
- Schuh, M., and Ellenberg, J. (2007). Self-organization of MTOCs replaces centrosome function during acentrosomal spindle assembly in live mouse oocytes. *Cell* *130*, 484–498.
- Schweizer, N., Pawar, N., Weiss, M., et al. (2015). An organelle-exclusion envelope assists mitosis and underlies distinct molecular crowding in the spindle region. *J. Cell Biol.* *210*, 695–704.
- Smyth, J.T., Beg, A.M., Wu, S., et al. (2012). Phosphoregulation of STIM1 leads to exclusion of the endoplasmic reticulum from the mitotic spindle. *Curr. Biol.* *22*, 1487–1493.
- Stein, D.S., and Stevens, L.M. (2014). Maternal control of the *Drosophila* dorsal-ventral body axis. *Wiley Interdiscip. Rev. Dev. Biol.* *3*, 301–330.
- Tashiro, F., Kanai-Azuma, M., Miyazaki, S., et al. (2010). Maternal-effect gene *Ces5/Ooep/Moep19/Floped* is essential for oocyte cytoplasmic lattice formation and embryonic development at the maternal-zygotic stage transition. *Genes Cells* *15*, 813–828.
- Tong, Z.B., Gold, L., Pfeifer, K.E., et al. (2000). Mater, a maternal effect gene required for early embryonic development in mice. *Nat. Genet.* *26*, 267–268.
- Xu, Q., Wang, F., Xiang, Y., et al. (2015). Maternal BCAS2 protects genomic integrity in mouse early embryonic development. *Development* *142*, 3943–3953.
- Yi, K., Rubinstein, B., Unruh, J.R., et al. (2013). Sequential actin-based pushing forces drive meiosis I chromosome migration and symmetry breaking in oocytes. *J. Cell Biol.* *200*, 567–576.
- Yu, C., Ji, S.Y., Sha, Q.Q., et al. (2016). BTG4 is a meiotic cell cycle-coupled maternal-zygotic-transition licensing factor in oocytes. *Nat. Struct. Mol. Biol.* *23*, 387–394.
- Yu, X.J., Yi, Z., Gao, Z., et al. (2014). The subcortical maternal complex controls symmetric division of mouse zygotes by regulating F-actin dynamics. *Nat. Commun.* *5*, 4887.
- Yurttas, P., Vitale, A.M., Fitzhenry, R.J., et al. (2008). Role for PADI6 and the cytoplasmic lattices in ribosomal storage in oocytes and translational control in the early mouse embryo. *Development* *135*, 2627–2636.
- Zheng, P., and Dean, J. (2009). Role of Filia, a maternal effect gene, in maintaining euploidy during cleavage-stage mouse embryogenesis. *Proc. Natl Acad. Sci. USA* *106*, 7473–7478.
- Zhu, K., Yan, L.Y., Zhang, X.X., et al. (2015). Identification of a human subcortical maternal complex. *Mol. Hum. Reprod.* *21*, 320–329.